Symposia D, E and F from MRS International Materials Research Conference IOP Publishing
Journal of Physics: Conference Series **152** (2009) 012026 doi:10.1088/1742-6596/152/1/012026

Reactively sputtered Ti-Si-N films for application as heating layers for low-current phase-change memory

You Yin, Tomoyuki Noguchi, Kazuhiro Ota, Naoya Higano, Hayato Sone, and Sumio Hosaka

Department of Production Science and Technology, Gunma University, 1-5-1 Tenjin, Kiryu, Gunma 376-8515, Japan

E-mail: yinyou@el.gunma-u.ac.jp

Abstract. In this study, we investigate the properties of Ti-Si-N films for the application as the heating layers in phase-change memory (PCM). The experimental results show that the resistivity of Ti-Si-N films can be varied by over six orders of magnitude from 2.18×10^{-4} to 3.9×10^{2} $\Omega\cdot\mathrm{cm}$ by increasing the flow rate ratio [$N_2/(N_2+Ar)$] from 0 to 10%. The controllability of resistivity might result from the concentration change from Ti-Si to mixture of TiN and Si_3N_4. Reversible switching was also successfully demonstrated by using a lateral PCM with these heating layers. The stability of the Ti-Si-N films at high temperatures implies that they can be used as the heating layers in the conventional vertical PCMs for current reduction.

1. Introduction

These guidelines, Phase-change memory (PCM) is widely regarded as the most promising non-volatile memory (NVM) substitute for the current flash memory [1-5]. PCM is based on the large resistivity difference between amorphous and crystalline phases, which can be reversibly transformed by the application of pulses of the order of ns [1, 4]. Although PCM as an NVM technology has almost perfect properties such as excellent endurance, direct overwriting, huge read dynamic range, fast speed, high performance, multi-state storage [7-8], and so on, its high programming current is the most important issue for its commercialization since its invention in 1960s [9-10].

Solutions to the issue of the high programming current mainly include selection or change of phase-change (PC) materials based on material properties and structure optimization [11-12]. Particularly, the programming current is expected to be greatly reduced due to the thermal confinement by introducing a heating layer such as GeN, SiGe, SiGeN and TiON into the conventional bottom contact PCM structure [13-15].

Furthermore, a lot of PC films except the intensively researched $Ge_2Sb_2Te_5$ were proposed and exhibited good performance in recent years [16-18]. These materials in poly-crytalline phase have a resistivity of $10^{-4}-1\,\Omega\cdot\mathrm{cm}$, one-to-two orders of magnitude either higher or lower than that of $Ge_2Sb_2Te_5$, i.e., around $10^{-2}\,\Omega\cdot\mathrm{cm}$. Further reducing the programming current of the PCM with these PC materials must optimize device structure, for example, inserting a heating layer close to PC layers. Correspondingly, heating materials with a very wide range of resistivity, for example,

$10^{-3} - 10^{2}\ \Omega\cdot\mathrm{cm}$, should be developed for these PC films. As far as we know, there is lack of such a universal heating material for PCM application.

In this study, we report the controllability of resistivity of TiSiN films by N_2 partial flow rate during reactive sputtering and how great the effect of the resistivity of the heating layer in PCM has on the programming current.

2. Experimental

Ti-Si-N films with a SiO_2 capping layer on glass substrates were prepared by simultaneously introducing N_2 and Ar into the chamber when sputtering. The radio-frequency sputtering equipment (MNS-3000-RF, ULVAC, Inc.) was adopted. The schematic diagram is shown in Fig. 1. Six Si chips (around 10×10 mm^2) were mounted on the Ti target. The sputtering conditions are as follows: a background pressure below 5×10^{-5} Pa, a sputtering pressure of 0.2 Pa and a power of 100 W. Flow rate ratio of $N_2/(N_2+Ar)$ increased from 0 to 10%. The total gas flow rate of (N_2+Ar) was set to be 10 sccm.

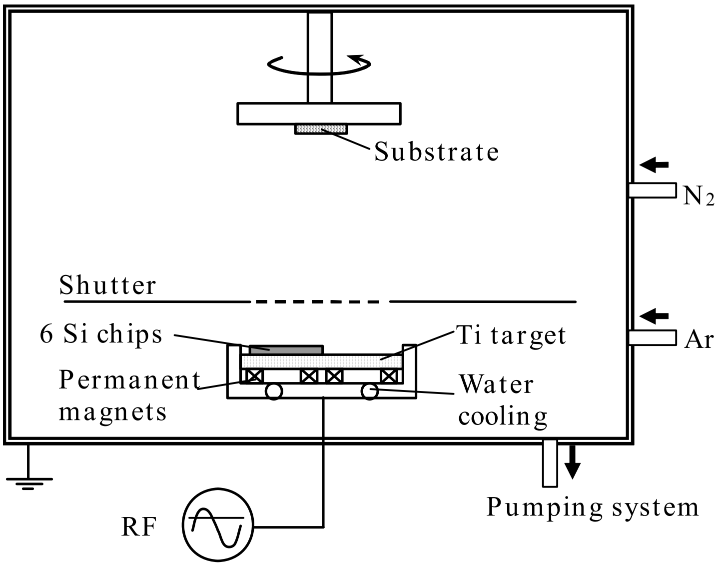

Fig 1. Schematic diagram of reactive RF magnetron co-sputtering apparatus.

The crystal structures of these films were characterized by means of an X-ray diffractometer (RINT 2000, Rigaku Co.) after the films were annealed on a hot plate up to 400°C for 5 min. The resistivity, as a function of the annealing temperature of the films annealed in the same way, was measured using square-shaped film samples defined by Ti electrodes.

The current-voltage (*I-V*) characteristics of the device samples were measured by a semiconductor parameter analyzer (4155B, Agilent Technologies, Ltd.). A waveform generator (Model 2571, Tabor Electronics, Ltd.) was used to apply single pulses to the devices.

3. Results and discussion

Sputtering rate of the Ti-Si-N films was determined by atomic force microscope (AFM) in the profile mode. It slightly decreases with increasing N_2 percentage in the mixed gas as shown in Fig. 2. Typical scanning electronic microscope (SEM) images are shown in Fig. 3. All of these reactively sputtered films were very smooth.

Resistivity of Ti-Si-N films with increasing N_2 percentage in the mixed gas as shown in Fig. 4 was investigated. The resistivity of the Ti-Si film (N_2: 0%) exhibits a very low resistivity of $2.18\times10^{-4}\ \Omega\cdot\mathrm{cm}$, which is very close to the reported data. It can be seen that increasing N_2 percentage from around 5% to 10% in the mixed gas can effectively control the resistivity of the Ti-Si-

N films. A resistivity with a very wide range of $5.7\times10^{-3}-3.9\times10^{2}\ \Omega\cdot\mathrm{cm}$ is available by simply adjusting the N_2 partial flow rate in the range of 5-10%. The resistivity of Ti-Si-N films increases with a strong dependence on flow percentage ($N_2/(N_2+Ar)$). One percentage of the increase in flow percentage ($N_2/(N_2+Ar)$) from 5% to 10% causes around one order of magnitude of resistivity increase.

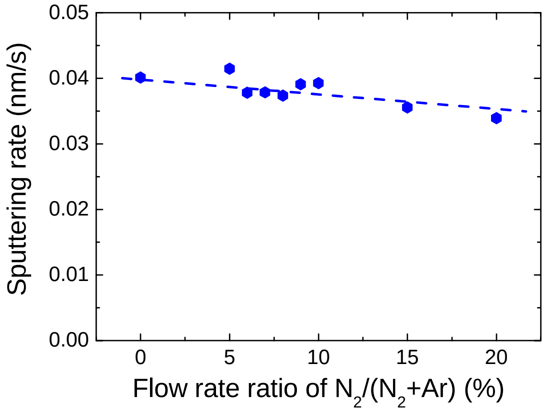

Fig 2. Sputtering rate as a function of the flow rate ratio of $N_2/(N_2+Ar)$.

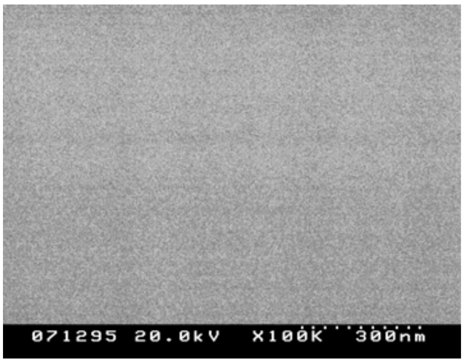

Fig 3. SEM images of Ti-Si-N film with the flow rate ratio ($N_2/(N_2+Ar)$) of 9%.

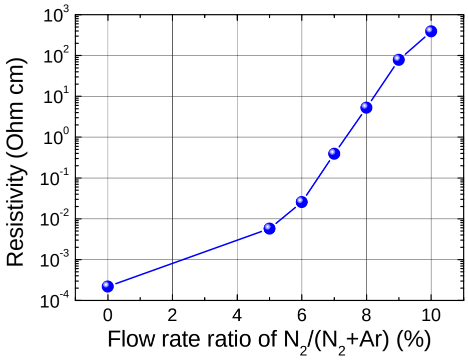

Fig 4. Resistivity of Ti-Si-N films as a function of the flow rate ratio of $N_2/(N_2+Ar)$.

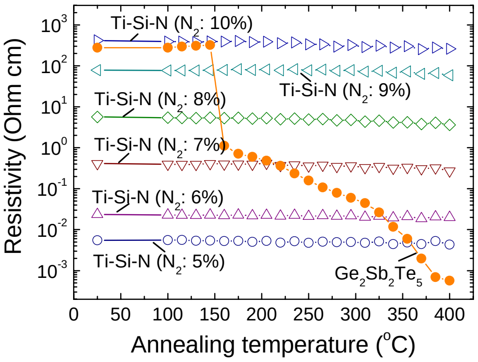

Fig 5. Resistivity of TiSiN and $Ge_2Sb_2Te_5$ films as a function of annealing temperature.

The effect of annealing on the resistivity was investigated and is shown in Fig. 5. The resistivity of $Ge_2Sb_2Te_5$ (GST, most widely used in PCM) films is also plotted for reference. Compared with the marked change in resistivity of $Ge_2Sb_2Te_5$ due to phase transformations, all of these Ti-Si-N films showed relative stability with temperature. Ti-Si film (N_2: 0%) has a very low resistivity of around $2.18\times10^{-4}\ \Omega\cdot\mathrm{cm}$, which is approximately the resistivity of hexagonal GST. When the flow percentage ($N_2/(N_2+Ar)$) increases to 6%, the resistivity of Ti-Si-N films increases up to the order of $10^{-2}\ \Omega\cdot\mathrm{cm}$, corresponding to that of the crystalline GST with a face-centered cubic structure. The resistivity of Ti-Si-N films (N_2: 10%) reaches up to 390 $\Omega\cdot\mathrm{cm}$, which is a little higher than that of amorphous GST.

Furthermore, thickness as a function of annealing temperature of the Ti-Si-N films was studied and showed weak temperature dependence as shown in Fig. 6. This implies that the properties of Ti-Si-N films are thermally stable.

M-Si-N (M= Mo, Ta, Ti, or W) films were investigated in the past years for application to the barrier materials for Al as well as Cu metallizations [19-21]. Although some papers revealed that the resistivity variation of the films is mostly effected by the film composition, a maximum resistivity is usually the order of 1 mΩ cm, which can not meet the requirements of the heater in PCM. These Ti-Si-N films are composed of TiN nanocrystalline grains and Si_3N_4 amorphous phase according to analysis. However, the X-ray diffraction patterns of our sputtered Ti-Si-N films after annealing show no peaks of TiN as shown in Fig. 7. This means that the Ti-Si-N films in this study might be composed of amorphous TiN and Si_3N_4. The composition and resistivity of the Ti-Si-N films are expected to be relatively stable even above the melting of PC materials (500-635°C) because of the very high crystallization temperature of TiN and Si_3N_4. The controllability of resistivity of the Ti-Si-N as shown in Fig. 4 is assumed to be based on the change of volume percentage of Si_3N_4 in the films.

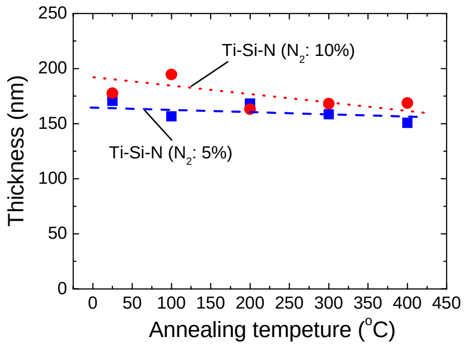

Fig 6. Thickness of TiSiN films as a function of annealing temperature.

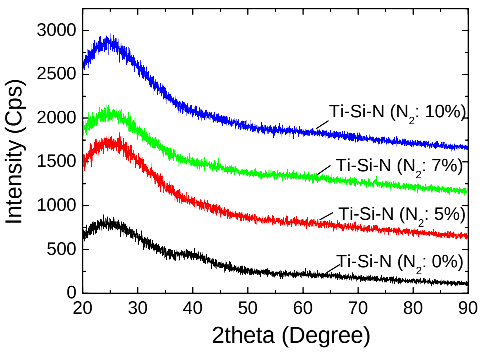

Fig 7. XRD patterns of Ti-Si and Ti-Si-N films.

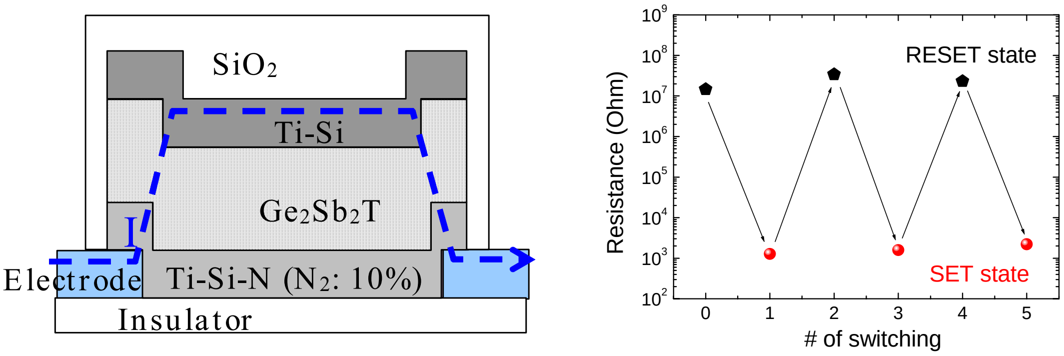

(a) (b)

Fig 8. (a) Schematic diagram of a lateral PCM with Ti-Si-N layers. (b) Resistance change as a function of the switching number.

To know if the Ti-Si-N films are possible to apply to PCM, a lateral PCM as shown in Fig. 8(a) was adopted for the testing of the stability of Ti-Si-N films at high temperature. In the channel between two electrodes, the GST layer was sandwiched with the top Ti-Si and the underlying Ti-Si-N

(N_2: 10%) layers. The current flows as shown by the dashed line. From Fig. 8(b), the device with Ti-Si-N layers can be reversibly switched between high-resistance amorphous set and low-resistance crystalline reset states. This means that the Ti-Si-N layers are able to be used as a heating layer in PCM because they can remain stable even at the high temperature above the melting point of GST (632 °C) during switching.

Next, we will show the effect of the resistivity of the heating layer on the reset current of the today's widely researched vertical PCM cell, which was simulated by finite element method. The PCM cell is assumed to have a Si substrate/W/TiN contact/additional heating layer/PC/W-layered structure as shown in the inset of Fig. 9. The thicknesses of all the layers from the bottom W layer are 50, 200, 5, 80, and 50 nm. The reset current can dramatically drop from 1.4 mA to several tens of μA by adopting a resistive heater for the resistivity of crystalline GST of $10^{-2}\ \Omega\cdot\mathrm{cm}$ as shown in Fig. 9.

The simulation results suggest that a heater with a resistivity of one-to-two orders of magnitude is very effective to further reduce the reset current without a significant drop in the difference in device resistance between set and reset states. As a result, the resistivity of the material used for a resistive heater is expected to have a wide range of around $10^{-3} - 10^{2}\ \Omega\cdot\mathrm{cm}$ if we take the practical PC materials with a resistivity of $10^{-4} - 1\,\Omega\cdot\mathrm{cm}$ into account. The resistivity of Ti-Si-N films can enter into the required range.

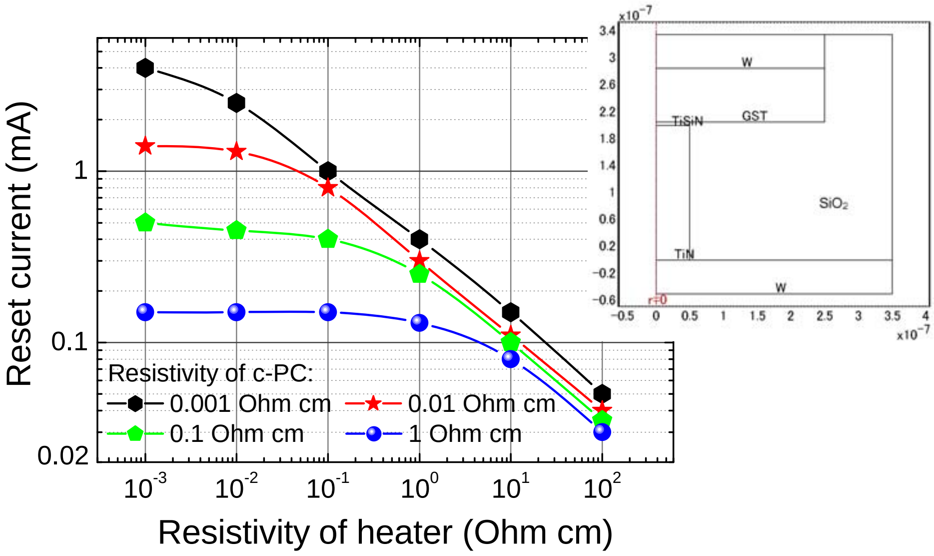

Fig 9. Reduction in reset current with increasing the resistivity of the Ti-Si-N heating layer.

4. Conclusions

In summery, Ti-Si-N films showed a controllable resistivity window from 2.18×10^{-4} to 390 $\Omega\cdot\mathrm{cm}$ and its good thermal stability. It is promising for Ti-Si-N films to be applied to the future's phase-change memory for reducing its operation current.

Acknowledgements

The authors would like to thank for financial support by Semiconductor Technology Academic Research Center (STARC) of Japan.

Reference

[1] S. Lai: Tech. Dig. IEDM, 2003, p. 255.
[2] Y. Yin, D. Niida, K. Ota, H. Sone, and S. Hosaka: Rev. Sci. Instrum. **78** (2007) 126101.
[3] H. Y. Cheng, Y. C. Chen, R. J. Chung, and T. S Chin: Semicond. Sci. Technol. **21**(2006) 1196.
[4] Y. Yin, A. Miyachi, D. Niida, H. Sone and S. Hosaka: Jpn. J. Appl. Phys. **45** (2006) L726.
[5] K. Nakayama, K. Kojima, F. Hayakawa, Y. Imai, A. Kitagawa, and M. Suzuki: Jpn. J. Appl. Phys. **39** (2000) 6157.
[6] Pirovano, A. L. Lacaita, A. Benvenuti, F. Pellizzer, and R. Bez: IEEE Trans. Electron Devices **51** (2004) 452.
[7] Y. Yin, H. Sone, and S. Hosaka: Microelectron. Eng. **84** (2007) 2901.
[8] F. Rao, Z. Song, M. Zhong, L. Wu, G. Feng, B. Liu, S. Feng, and B. Chen: Jpn. J. Appl. Phys. **46** (2007) L25.
[9] D. H. Kang, D. H. Ahn, K. B. Kim, J. F. Webb, and K. W. Yi: J. Appl. Phys. **94** (2003) 3536.
[10] Y. Yin, H. Sone, and S. Hosaka: Jpn. J. Appl. Phys. **45** (2006) 8600.
[11] Y. H. Ha, J. H. Yi, H. Horii, J. H. Park, S. H. Joo, S. O. Park, U. I. Chung, J. T. Moon: Symp. VLSI Tech. Dig. Tech. Pap., 2003, p. 175.
[12] Y. Yin, H. Sone and S. Hosaka: Jpn. J. Appl. Phys. **45** (2006) 6177.
[13] J. Shen, B. Liu, Z. Song, C. Xu, F. Rao, S. Liang, S. Feng, and B. Chen: Applied Physics Express, **1** (2008) 011201.
[14] D. H. Kang, D. H. Ahn, M. H. Kwon, H. S. Kwon, K. B. Kim, K. S. Lee, and B. Cheong: Jpn. J. Appl. Phys. **43** (2004) 5243.
[15] S. Y. Lee, K. J. Choi, S. O. Ryu, S. M. Yoon, N. Y. Lee, Y. S. Park, S. H. Kim, S. H. Lee, and B. G. Yu: Appl. Phys. Lett. **89** (2006) 053517.
[16] Y. Ling, Y. Lin, B. Qiao, Y. Lai, J. Feng, T. Tang, B. Cai and B. Chen: Jpn. J. Appl. Phys. **45** (2006) L349.
[17] K. Nakayama, K. Kojima, Y. Imai, T. Kasai, S. Fukushima, A. Kitagawa, M. Kumeda, Y. Kakimoto and M. Suzuki: Jpn. J. Appl. Phys. **42** (2003) 404.
[18] Y. Yin, H. Sone, and S. Hosaka: J. Appl. Phys., **102** (2007) 064503.
[19] J. S. Reid, E. Kolawa, C. M. Garland, M. A. Nicolet, F. cardone, D. Gupta and R. P. Ruiz: J. Appl. Phys., **79** (1996) 1109.
[20] W. H. Lee, S. K. Park, B. J. Kang, P. J. Reucroft, and J. G. Lee: J. Electronic Materials, 30 (2001) 84.
[21] X. Sun, J. S. Reid, E. Kolawa, and M. A. Nicolet: J. Appl. Phys., **81** (1997) 656.